

# Dynamic Contrast Ultrasound Diagnostics (CEUS) of Liver Lesions and Post-treatment Control with A New High-resolution Examination Technique (HiFR) and Perfusion

Ernst Michael Jung<sup>1</sup>, Lukas Pleyer<sup>1</sup>, Ivor Dropco<sup>2</sup>, Ulrich Kaiser<sup>3</sup>, Dong Yi<sup>4</sup>, Christian Stroszczyński<sup>1</sup>, Friedrich Jung<sup>5</sup>

1) Institute of Diagnostic Radiology, Interdisciplinary Ultrasound Department, University Hospital Regensburg, Regensburg, Germany;  
 2) Department for Surgery, University Hospital Regensburg, Regensburg, Germany;  
 3) Clinic and Polyclinic for Internal Medicine III, University Hospital Regensburg, Regensburg, Germany;  
 4) Department of Ultrasound Zhongshan Hospital, Fudan University, Shanghai, China;  
 5) Institute of Biotechnology, Molecular Cell Biology, Brandenburg University of Technology Cottbus-Senftenberg, Senftenberg, Germany

## Address for correspondence:

### Ivor Dropco

Department for Surgery,  
 University Hospital  
 Regensburg, Regensburg,  
 Germany  
 ivor.dropco@ukr.de

Received: 12.03.2024

Accepted: 13.05.2024

## ABSTRACT

**Background & Aims:** To evaluate, if high frame rate (HiFR) contrast-enhanced ultrasound (CEUS) and external perfusion analysis (VueBox®) can give answers on liver tumour diagnostics.

**Methods:** A multifrequency probe (C1-6 /Resona R9) and 1-2.4 ml ultrasound contrast medium were used for CEUS up to 5-6 min. Independent analysis of DICOM-CINE files was performed, correlated to follow-up, computed tomography, magnetic resonance imaging, or histopathology.

**Results:** In 110 patients the difference between marginal peak enhancement (PE) of malignant and benign lesions was significant. In the peripheral area, the AUCs were lower in malignant lesions (144.8±139.3) than in benign lesions (123.6±119.8). The mean transit time (mTT) was shorter in malignant lesions in the center. In the liver parenchyma, however, the mTT was significantly longer in malignant lesions (141.6±107.9s) than in benign lesions (128.8±138.6 s). The rise time (RT) was significantly shorter central (66.5±30.9s) and peripheral (72.8±35.1s) in malignant lesions than in benign lesions (114.33±159.58s). The wash in rate (WiR) in benign lesions was 848.3±2,563.7 rU in the center. Wash-out rate (WoR) in the center, peripheral and in the liver parenchyma showed a significantly lower wash-out in the malignant lesions.

**Conclusions:** HiFR CEUS with perfusion analysis enables the assessment of focal, diffuse and post-interventional liver changes.

**Key words:** liver ultrasound – CEUS – Perfusion – VueBox® analysis – tumour diagnostics – post ablation defects.

**Abbreviations:** AUC: Area under the Curve; CCC: cholangiocarcinoma; CDDS: colour-coded duplex sonography; CEUS: contrast-enhanced ultrasonography; CHI: contrast harmonic imaging; CT: computed tomography; ECT: electrochemotherapy; FNH: focal nodular hyperplasia; GEN: General; HCC: hepatocellular carcinoma; HiFR: high frame rate; MRI: magnetic resonance imaging; mTT: mean transit time; NET: neuroendocrine tumor; PEAK: peak enhancement; PEN: Penetration; PIHI: pulse inversion techniques; RES: Resolution; ROI: region of interest; RT: rise time; TACE: transarterial chemoembolization; THI: tissue harmonic imaging; TTP: time to peak; VueBox®: external perfusion analysis; WiR: wash in rate; WoR: wash-out rate.

## INTRODUCTION

Contrast-enhanced ultrasonography (CEUS) of the liver has become an indispensable diagnostic tool [1–3]. In a large-scale study, CEUS has already demonstrated a diagnostic reliability comparable to that of contrast-enhanced computed tomography (CT) with regard to the characterization of solid liver lesions [4]. In comparison to contrast-enhanced magnetic

resonance imaging (MRI), the use of liver-specific MRI contrast agents may result in diagnostic advantages compared to CEUS with regard to the detection and evaluation of solid liver lesions.

A continuous development can also be observed with the ultrasound contrast agent used. Second-generation ultrasound contrast agents are based on the principle of echo signal amplification through the oscillation of microbubbles using contrast harmonic imaging (CHI). International guidelines describe a variety of applications for diagnostic use in the liver [5, 6].

The potential side effects of CEUS are considered to be not critical. This is in line with the continuous increase in the clinical use of this technique. Ultrasound contrast agents do not impair kidney or thyroid function. If the function of

these organs is too impaired for the use of CT/MRI contrast agents, CEUS diagnostics can therefore be a good diagnostic possibility [7, 8].

In Europe, the ultrasound contrast agent SonoVue® (BRACCO/Italy) is most commonly used. This is based on sulphur hexafluoride microbubbles. Administration takes place via intravenous bolus injection. Similar to the contrast enhanced MRI technique, there is an ongoing development of liver-specific ultrasound contrast agents. However, these are currently only available in isolated cases and not in all countries.

Many of modern developments have been made to improve CEUS technology. These include: high-resolution multi-frequency probes (especially sector or lin-ear transducers) equipped with an increasing number of crystals; modified CHI programmes [including enhanced amplitude modulation and pulse inversion techniques (PIHI)]; enhanced digital image storage (e.g. of CINE sequences); optimization of frame rates for greater resolution and accuracy. One possible new contrast medium ultrasound technique that attempts to utilize all these advantages is the high rate frame (HiFR) technique [2].

With an additional perfusion analysis from the early arterial phase to the portal venous phase, i.e. during the first minute after contrast medium injection, an independent analysis of the dynamic microcirculation of liver lesions can be performed using DICOM files. Using special external software (VueBox®/Bracco), a comprehensive assessment of the wash-in and wash-out kinetics of liver lesions is possible.

Whether there are diagnostic advantages for CEUS with a novel examination mode HiFR and external perfusion analysis must be analyzed independently in comparison to the diagnostic safety of reference imaging such as contrast-enhanced CT or MRI (if histopathology is not available).

In the present study, the extent to which the new HiFR technique supplemented by dynamic perfusion analysis in the arterial and portal venous phase can be used for reliable CEUS diagnostics of complicated cystic, solid benign and malignant tumours, ablation defects and microcirculatory disorders in the liver was examined.

## METHODS

Written consent was obtained from all patients. The evaluation was carried out independently using the image data stored in the PACS by experienced readers in consensus. An ethics vote from the Ethics Committee of the University Hospital Regensburg (vote number: 22-3128-104) is available for the scientific evaluation of the contrast agent sonography data for the diagnosis of liver lesions. The CEUS liver tumour diagnostics technique complies with the specifications of the DEGUM studies.

In this retrospective study, the sonographic examination results of 110 patients were analyzed as DICOM loops and divided into three groups according to the pathology present. The first group consisted of patients with malignant liver lesions. The second group consisted of patients with benign liver disease. The third group included patients who had undergone an intervention [microwave ablation (MWA), resection, transarterial chemoembolization (TACE),

electrochemotherapy (ECT), radiofrequency ablation (RFA)] for a previous malignant disease.

The purpose of the examinations was to further clarify unclear liver lesions on the basis of the available diagnostic findings. The endpoints of the CEUS examination were a definitive diagnosis, type/localisation and number of liver lesions as well as perfusion changes. In the case of definitive benign findings, a follow-up examination was performed after 3-6 months. In the case of suspected malignant lesions [e.g. hepatocellular carcinoma (HCC) or cholangiocellular carcinoma (CCC)], a classification according to LI-RADS IV-V was carried out according to the probability of malignancy. A corresponding expansion of diagnostic imaging was also initiated. If there was evidence of metastases, a primary tumour search was, initiated including a potentially necessary biopsy. If available, a comparison was made with the surgical result of a liver tumour resection.

The analyses were carried out by a high experienced ultrasound specialist (DEGUM Level III) with a multi-frequency convex probe (C1-6 MHz) on a high-end ultrasound device (Resona R9/7, Mindray). Detectable lesions were documented in B-mode (2 planes). Optimisation (depth-dependent via frequency) and the use of other supplementary techniques [Tissue Harmonic Imaging (THI), ultrasound CT technique and averting photopic technique (B-Colour)] were also performed. Liver macrovascularisation was performed using colour-coded duplex sonography (CCDS). Optimising techniques were also used here (e.g. HR flow technique, glazing flow, optimisation of the wall filter and colour enhancement settings).

Diagnostic clues in CDDS were a spoke wheel pattern in focal nodular hyperplasia (FNH), marginal vascularization in adenomas (hepatic adenoma) or irregular central vascularization in HCC. Vascular tumour infiltration also had to be detected, particularly in relation to the hepatic veins and the portal vein intrahepatically. In the case of vascular changes, the CCDS was used to detect shunts or vascular rupture in embolisms and infarcts.

The CEUS examination was performed by intravenous bolus administration of the ultrasound contrast agent (SonoVue). Prior to administration, a critical assessment was made with regard to potential contraindications (e.g. known contrast agent intolerance). This was based on the EFSUMB guidelines. The examinations were carried out dynamically using the HiFR technique with subsequent digital documentation. The modalities used were General (GEN), Resolution (RES) or Penetration (PEN).

The sweep method was also used. A continuous recording of the arterial phase after 10 to 15 s after bolus administration up to the portal venous phase over 1 minute and in the case of vascular changes with optimal recording of the liver hilus in order to be able to detect possible arteriovenous or portal venous macro- or microshunts was carried out. These continuous CEUS cine loops of contrast enhancement up to a possible early wash out over 1 minute after bolus injection were then exported as DICOM files for independent perfusion analysis with external perfusion software (VueBox®/Bracco). After motion correction, various perfusion parameters were analyzed, such as time to peak (TTP), peak enhancement (PEAK), mean transit time (mTT), rise time (RT), wash-in

and possible wash-out kinetics with linear and fit plots. For this purpose, the center, the edge and the reference liver tissue were initially marked in round regions of interest (ROIs) with a maximum diameter of 5 mm, then individually adapted in a ring shape for 3 independent evaluations. The measured values were documented in a measurement protocol and in tabular form. A perfusion curve was calculated using time intensity curve analysis of peak enhancement and the different perfusion parameters were displayed in false colours, with red representing maximum values, followed by orange, yellow, green, light blue to minimum dark blue to violet.

From the first minute after bolus administration, the CEUS was used to document a possible wash-out. Short cine loops of 5 to 10 s up to a late phase of 5 to 6 minutes were used. In addition, single images were added, which could be saved during the cine sequences in relation to the findings.

According to the EFSUMB Guidelines/DEGUM studies, continuous contrast enrichment in CEUS, marginal nodular enhancement, regular marginal contrast enrichment were considered typical for benign lesions such as FNH, typically with central scar, hemangiomas and adenomas. Classical for malignant lesions (e.g. metastases, CCC, HCC) was an irregular arterial vascularization with increasing washout of the tumor lesions in the late phase, in metastases already in the portal venous phase, in HCC often only after 3 minutes, in CCC in between. In the case of complicated cysts, attention was paid to a possible contrast agent enrichment of the septa. In the case of vascular alterations, the reference was the contrast of the unaffected liver tissue and the contrast of the hepatic artery, portal vein and hepatic veins.

An onward flow 20 s. Typical for shunts was a contrast of the portal vein after 20 s and the hepatic veins after 30 s. After completion of the documentation of the late phase, this could then be checked after 5 to 6 minutes using the technique of replenishment (FLASH kinetics) specifically for specific liver segments by detecting a re-flooding of the microbubbles to determine how extensive the shunts were. If necessary, the hemodynamics were then specifically assessed again with the CCDS. Follow-up with CEUS for benign lesions was carried out (after 3 to 6 months). Malignancy was verified by reference imaging (CT, MRI, biopsy or surgery).

For CT, multi-slice CT examinations in the arterial and portal venous contrast phases would be the reference with 80 to 120 ml of iodine-containing contrast agent in 5 mm axial and coronary reconstructions would be the reference, taking into account possible contraindications. MRI was performed on latest generation 1.5 and 3 Tesla scanners with native T1 and T2 sequences in 5 mm slices, diffusion sequences with b-values up to 1800 and ADC evaluation, and with liver-specific contrast agents (Primovist®) as 3D vibratory sequences in 3 mm reconstructions.

Liver biopsies were performed on an inpatient basis, and with written informed consent given 24 hours prior to the procedure and with all safety measures in place. After surgical disinfection under sterile conditions using a 16 G semi-automatic biopsy needle, representative cylinders of up to 2 cm in length were taken from the tumour area under US guidance using a puncture line and a second sample was taken from the peripheral tissue.

### Statistical Analysis

Statistical analysis was performed using the statistical software Datatab statistical software. All samples were described by mean and standard deviation.

Differences between benign and malignant lesions were determined using the Mann-Whitney U-Test. The null hypothesis was that there were no differences between the two samples. Probabilities less than 0.05 were considered significant.

## RESULTS

An overview of malignant and benign liver lesions examined is listed in Table I.

**Table I.** Malignant and benign liver lesions examined with a VueBox®

Malignant liver lesions n = 31	Type of the lesion	Number in n
	HCC	11
	CCC	5
	Metastasis	13
	Adenocarcinoma	1
	Leiomyosarcoma	1
Benign liver lesions n = 46	Hemangioma	11
	FNH	7
	Avascular Cyst	8
	Abscess	1
	Osler's disease	9
	Fat distribution disorder	3
	Parasitosis	1
	Polyp/adenomyomatosis	2
	Adenoma	1
	Multiple myeloma	1

Overview of malignant and benign liver lesions examined with a VueBox®. HCC: hepatocellular carcinoma; CCC: cholangiocellular carcinoma; FNH: focal nodular hyperplasia.

In all cases, CEUS was technically feasible with good image quality in 52% (4 points) and very good image quality in 27% (5 points). Due to difficult sound conditions, such as meteorism, colonic interposition, inhomogeneous marked steatosis hepatitis in adipositas per magna, and due to movement instability, the digital cine sequences were limited in image quality in 13% of cases, but the image quality was still sufficient (rating of 3 points). In only 2% of cases with extremely difficult sound conditions for segment VIII lesions, the image quality was significantly impaired by distances to the lesions > 20 cm (scored 2 points).

On MRI, respiratory artefacts, especially in the late contrast sequences, resulted in reduced image quality (< 3 points) in 20% of patients. In 15% of CT scans, inhomogeneous contrast enhancement was observed due to mixed contrast enhancement of the liver, even when faster multislice techniques were used.

The DICOM loops of 31 patients (age 18 to 78 years, mean 57 years, 24 males, 7 females) with different malignant liver lesions were examined and evaluated with the VueBox®.

The malignant lesions were either primary liver tumours or secondary liver tumours in the sense of metastasis from a primary tumour in other organs (HCC n=11, CCC n=5, metastases n=13, adenocarcinoma n=1, leiomyosarcoma n=1). The most frequently involved segments were V, VI and VII. The examined malignant lesions of group 1 had a mean size of 6.7 cm with a distribution of (0.3±13 cm).

The patient cohort of benign lesions consists of the DICOM loops of 46 patients (age 18 to 85, mean 55 years, 27 females, 19 males) with various benign liver lesions. These were examined and evaluated using the VueBox®. The benign lesions were various benign diseases of the liver, including both benign tumours and vascular diseases (hemangioma n=11, FNH n=7, avascular cyst n=8, abscess n=1, Osler’s disease n=9, fat distribution disorder n=3, parasitosis n=1, polyp/adenomyomatosis n=2, adenoma n=1, multiple myeloma n=1). The examined benign lesions had a mean size of 21.2 cm with a distribution of (0.2±42 cm). The most frequently involved segments were II, V and VIII.

In the post-interventional liver lesion patient cohort, the DICOM loops of a total of 33 patients with malignant liver lesions were examined after intervention and evaluated with the VueBox®. The interventions included ablations, resections, TACE and ECT. This group was further divided into a post-interventional group with residual tumour (10 metastases, 3 CCC, 2 HCC) with control after MWA n=8, ECT, n=3, resection n=2, TACE+RFA n=2) with 15 patients each (42 to 81 years, mean 55 years, 9 female, 6 male). The most commonly affected segments were V and VI. The examined malignant postinterventional lesions of group 3a had a mean size of 2.3 cm with a distribution of (0.5 to 4.5 cm).

In the postinterventional group without residual disease (HCC n=13, CCC n=3, metastases n=2) after MWA n=12, irreversible electroporation IRE n=2, ECT n=2, resection n=2) were 18 patients (age 51 to 87, mean 51 years, 14 male, 4 female), the most common localisations were segment II,

IV, VIII. The examined post-interventional lesions of the group without residual tumour had a mean size of 4 cm with a distribution of (3 to 5 cm).

The evaluation of PEAK was 14,270.81±16,672.07 relative unit (rU) for malignant lesions in the centre and 195.05±161.91 rU in the periphery compared with 353,343.93±557.141.43 rU for the liver parenchyma. Peak enhancement for benign lesions was 16,071.39±29,638.39 rU in the centre and 160.15±229.98 rU in the periphery compared with 836,628.64± 2,293,804.06 rU in the liver parenchyma. A Mann-Whitney U-test showed that the difference between PEAK rim malignant and PEAK rim benign with respect to the dependent variable was statistically significant p<0.01 (Table II).

A Mann-Whitney U-test showed that the difference between malignant TTP in the centre (72.16±32.11 s), in the periphery (74.94±31.53 s) and in the liver parenchyma (21, 3±10.7 s) and TTP in the centre (103.4±97.9 s), in the periphery (101.2±98.2 s) and in the liver parenchyma (20±10.7 s) not statistically significant, in the centre p=0.06 in the centre. When examining the parameter TTP, the absolute values in the centre and in the periphery of the examined regions showed a significantly shorter TTP in malignant lesions compared to benign lesions. When comparing normal liver parenchyma in malignant lesions with normal liver parenchyma in benign lesions, malignant lesions had a longer TTP than benign lesions.

When examining the Area under the Curve (AUC) parameter, there was a clear difference between malignant and benign lesions in the center of the examined regions. The AUC was significantly higher in the malignant lesions (176.1± 231.0) compared to the benign lesions (163.4±243.1). At the margin, the AUCs were lower in the malignant lesions (144.8±139.3) than in the benign lesions (123.6±119.8). The AUC values for liver tissue were lower in the malignant group (2,720,700.2±2,889,500.8) than in the benign lesions (3,632,376.15± 4,224,064.45). The Mann-Whitney U-test showed no significant statistical difference (p>0.05) between malignant and benign lesions for the AUC parameter.

**Table II.** Parameters measured for statistical analysis in different regions (central, periphery and liver tissue) for malignant and benign liver lesions

	Malignancy of FLL	Center	Periphery	Liver	p
Peak enhancement (rU)	Malignant	14,270.81±16,672.07	195.05±161.91	353,343.93±557.14	<0.01
	Benign	16,071.39±29,638.39	160.15±229.98	836,628.64± 2,293,804.06	
Time to peak (seconds)	Malignant	72.16±32.11	74.94±31.53	21, 3±10.7	<0.01
	Benign	103.4±97.9	101.2±98.2	20±10.7	
Area under the curve (rU)	Malignant	176.1± 231.0	144.8±139.3	2,720,700.2±2,889,500.8	>0.05
	Benign	163.4±243.1	123.6±119.8	3,632,376.15± 4,224,064.45	
Mean transit time (seconds)	Malignant	128.6±179.8	115.3±123.1	141.6±107.9	>0.05
	Benign	200.3 ± 293.3	161.5±203	128.8±138.6	
Rise time (seconds)	Malignant	66.5±30.9	72.7±35.1	16.2±7.4	<0.05
	Benign	114.3± 159.6	112.7±146.2	15.1±8.2	
Wash in rate (rU)	Malignant	385.8±320.8	290.04 ±202.7	97,202.0±328,762.02	<0.05
	Benign	848.3±2,563.7	369.2±958.8	411,737.6±2,098,161.9	

FLL: focal liver lesions; rU: relative units.

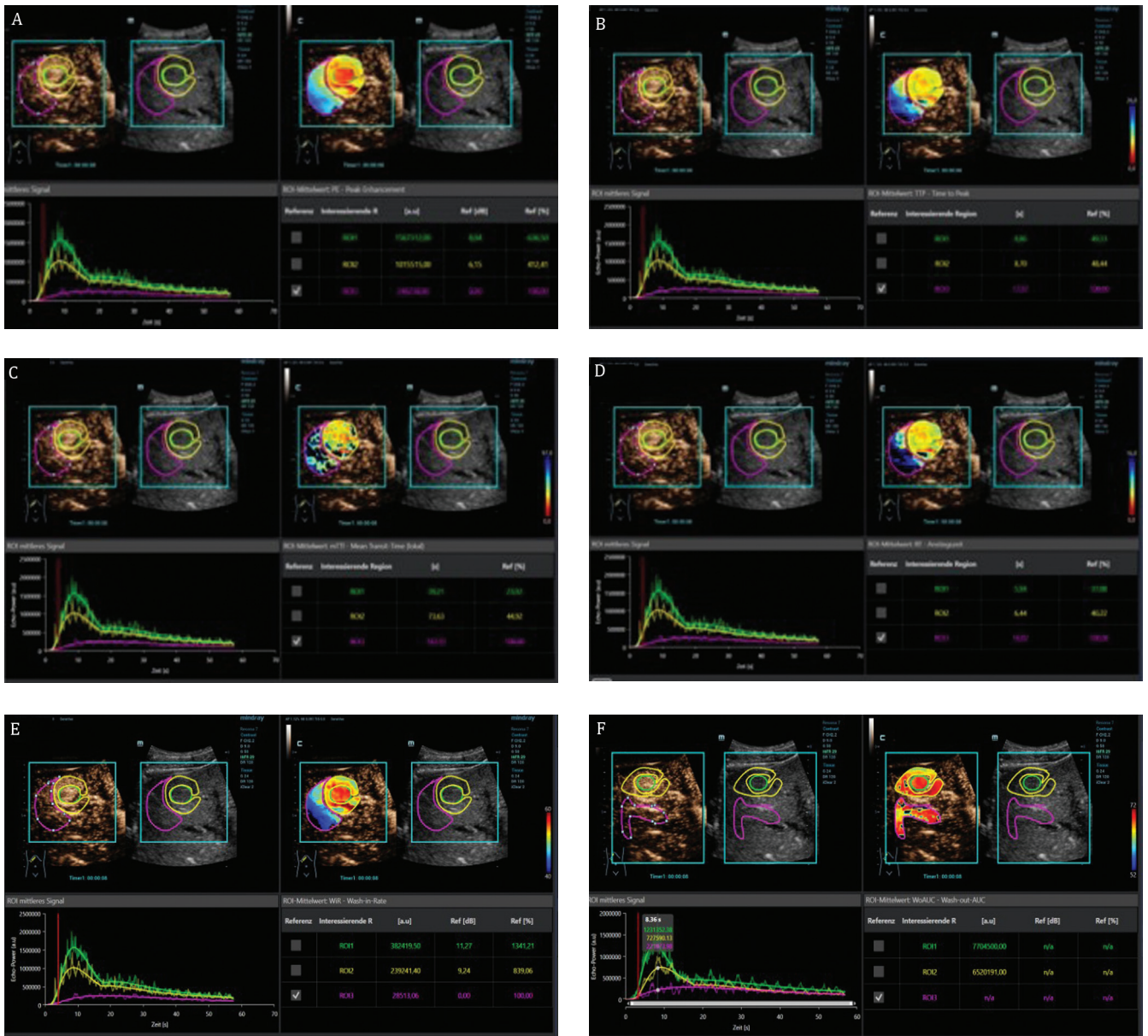


**Fig. 1.** Case of a small HCC lesions. HiFR-CEUS perfusion imaging using the VueBox®; Regions of interest (ROI) in the centre of the lesion (green), at the margin (yellow) in comparison with the liver tissue. Early and high enhancement and then the wash-out characteristic is typical for neovascularization of malignant liver lesions. A) evaluation of the peak enhancement (PE) with high values in the centre and at the margin. B) evaluation of the short time to peak (TTP) in the centre and at the margin. C) evaluation of the short mean transit time (mTT) in the centre and at the margin. D) evaluation of the short rise time (RT) in the centre and at the margin. E) evaluation of the wash-in rate with high values in the centre and at the margin. F) evaluation of the wash-in and wash-out kinetic.

When looking at the mTT, it can be seen that it is shorter in the center of malignant lesions ( $128.6 \pm 179.8$  s) compared to benign lesions ( $200.3 \pm 293.3$  s), as well as in the peripheral area of malignant lesions ( $115.3 \pm 123.1$  s) than in benign lesions ( $161.5 \pm 203$  s). In the liver parenchyma, however, the mTT is significantly longer in malignant lesions ( $141.6 \pm 107.9$  s) than in benign lesions ( $128.8 \pm 138.6$  s). The Mann-Whitney U test showed no significant statistical difference ( $p > 0.05$ ) between malignant and benign lesions for the mean transit time parameter.

When looking at the parameter RT, a significantly shorter RT can be observed in the center ( $66.5 \pm 30.9$  s) and in the peripheral area ( $72.7 \pm 35.1$  s) in malignant lesions, compared to

the RT in benign lesions in the center ( $114.3 \pm 159.6$  s) and in the peripheral area ( $112.7 \pm 146.2$  s). In the healthy liver parenchyma, however, the RT is slightly longer in malignant lesions ( $16.2 \pm 7.4$  s) than in benign lesions ( $15.1 \pm 8.2$  s). The Mann-Whitney U-test showed a significant statistical difference in the parameter Rise Time in the marginal area of the lesions ( $p < 0.05$ ).

The WiR in the center ( $385.8 \pm 320.8$  rU), in the periphery ( $290.04 \pm 202.7$  rU) and in the liver parenchyma ( $97,202.0 \pm 328,762.02$  rU) in malignant lesions showed a significantly lower WiR compared to benign lesions in the center ( $848.3 \pm 2,563.7$  rU), periphery ( $369.2 \pm 958.8$  rU) and liver parenchyma ( $411,737.6 \pm 2,098,161.9$  rU). A lower WiR was found to be a characteristic of the malignancy of the lesion.

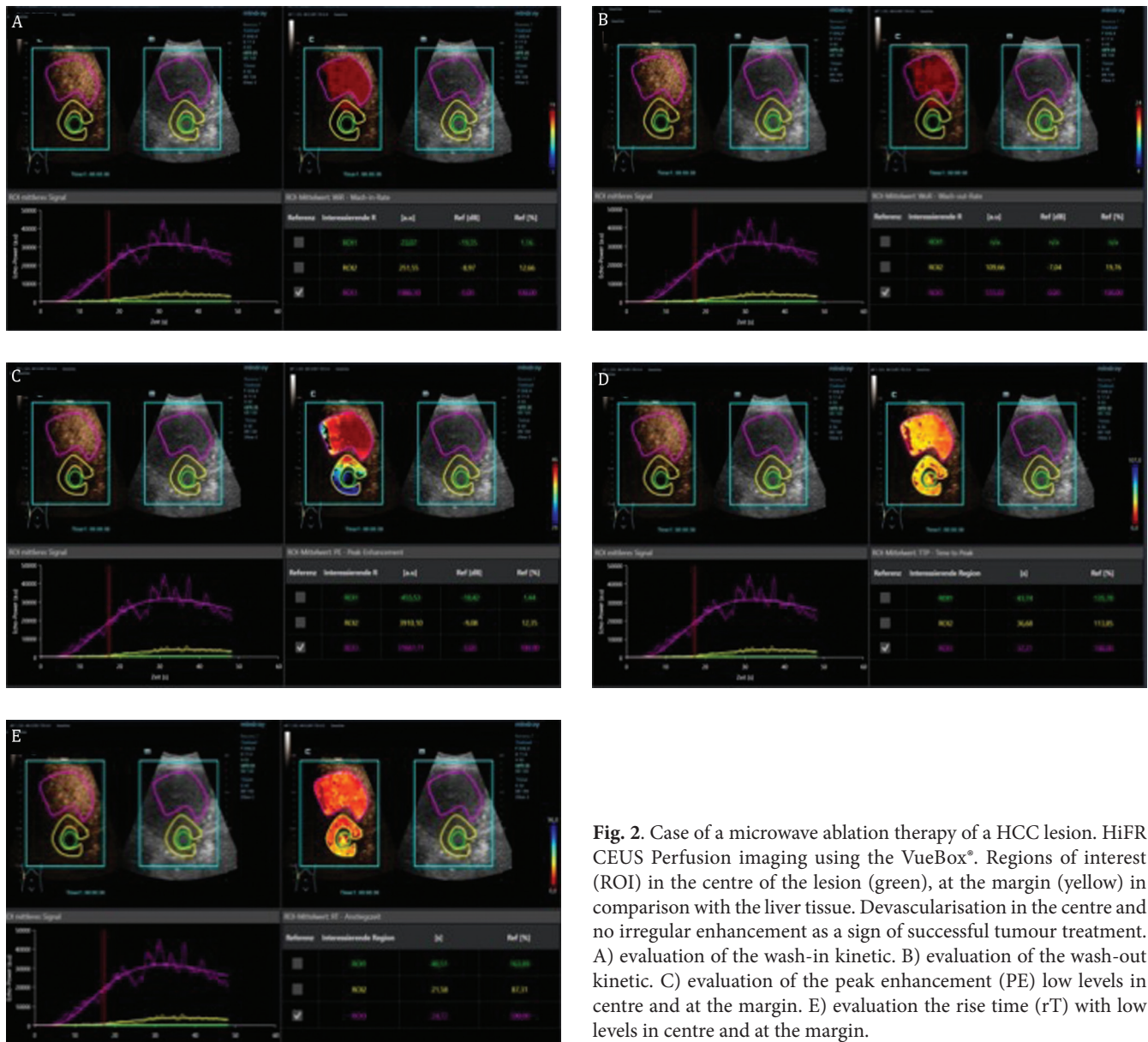


**Fig. 2.** Case of a microwave ablation therapy of a HCC lesion. HiFR CEUS Perfusion imaging using the VueBox®. Regions of interest (ROI) in the centre of the lesion (green), at the margin (yellow) in comparison with the liver tissue. Devascularisation in the centre and no irregular enhancement as a sign of successful tumour treatment. A) evaluation of the wash-in kinetic. B) evaluation of the wash-out kinetic. C) evaluation of the peak enhancement (PE) low levels in centre and at the margin. E) evaluation the rise time (rT) with low levels in centre and at the margin.

The Mann-Whitney U-test showed a significant statistical difference in the WiR parameter in the center and periphery of the lesions ( $p < 0.05$ ).

When looking at the WoR, both the center ( $581.71 \pm 595.78$  rU) and the peripheral area ( $321.1 \pm 197.6$  rU) and the healthy liver parenchyma ( $16,446.8 \pm 28,410.0$  rU) a significantly lower wash-out rate in the malignant lesions, compared to the benign lesions in the center ( $2,052.3 \pm 5,202.8$  rU), in the periphery ( $70,822 \pm 2,108.6$  rU) and liver parenchyma ( $905,601.3 \pm 3,728,728.6$  rU). The Mann-Whitney U-test showed a significant statistical difference in the WoR parameter in the marginal area of the lesions ( $p < 0.05$ ) (Table II).

With the HiFR CEUS, the typical contrast agent behavior from the edge to the center, nodular in the case of hemangiomas and from the center to the edge in the sense of a spoke wheel pattern in the case of FNH could be derived in all cases of benign liver lesions, such as hemangiomas and FNH, leading to a diagnosis. The contrast uptake increased in the late phase up to 5 min. The contrast uptake was complete in typical

hemangiomas, while a central recess remained in partially thrombosed atypical hemangiomas. In typical cases of FNH, a central scar was found.

The lack of contrast enhancement from the arterial to the late phase was typical for scarring changes after ablation (MWA) or postoperatively in CEUS.

In marginal recurrences, there would typically be an irregular nodular accumulation of contrast medium arterially in the marginal area and a wash-out of these nodular tumour parts beginning in the portal-venous phase.

With HiFR CEUS, the defects were correctly assessed in all cases. This was also the case for postoperative defects with localized reduced fat deposits. In these cases, the hypoechoic areas in the B-scan appear garland-shaped with wavy edges.

Magnetic resonance imaging examinations with dynamic contrast sequences (Vibe-3D) and diffusion sequences at 1.5 or 3 Tesla with specific contrast agent (Primovist®) or a 2-phase multislice CT with arterial and later portal venous phase served as a reference.

Typical for malignant lesions was an arterial irregular accumulation of contrast medium in the HiFR CEUS and a wash-out beginning in the portal venous phase and increasing towards the late phase. In all cases of colorectal metastases, detection that is more reliable was achieved in correlation with CT or MRI. However, evidence of irregular marginal vascularization was detectable for all lesions. However, it was possible to delineate the metastases with high image quality from as little as 5 mm in diameter using the wash-out in the portal venous phase after 60 s up to the late phase of 5 to 6 min. The image quality was in some cases better than CT and reached that of MRI with liver-specific contrast agent in almost all cases. In cases of small septated cysts up to 10 mm in diameter, HiFR CEUS proved to be superior to CT for differentiation from metastases.

In the detection of HCC or CCC, HiFR CEUS was successful in detecting the irregular, almost chaotic early hypervascularization of the tumour foci and the wash-out from the portal venous phase onwards; in the case of HCC, this was often only clearly visible in the late phase from 4 min onwards, if the tumour foci were > 15 mm in diameter, with good and very good image quality. In the case of several suspicious foci, the detection of all malignant lesions of a CCC or HCC in HiFR CEUS, especially the detection of small tumour foci > 10 mm in the late phase, is crucial. This was possible with HiFR CEUS in almost all cases with good image quality, in some cases even very good. The image quality was often significantly limited by the echo-inhomogeneous cirrhosis.

The assessment of tumour foci with a maximum diameter of only 10 mm was more difficult. Under difficult acoustic conditions, it can be difficult to assess both the hypervascularization and the partial wash-out as reliably malignant at a depth of < 15 cm. Therefore, one case was assessed as regenerative dysplastic with HiFR CEUS. In this case, the final assessment as an HCC lesion was made using MRI with liver-specific contrast agent.

## DISCUSSION

The results of the study emphasize that modern technical developments such as the HiFR perfusion analysis CEUS have the potential to enable a high level of diagnostic certainty with only a low risk in liver diagnostics [2, 9]. However, there are a number of relevant influencing factors that can affect the result. These include the examination conditions, patient compliance and the technical and practical capabilities of the examiner. Under favorable conditions, CEUS can achieve a diagnostic certainty of well over 90% in the detection and description of focal liver lesions and is therefore comparable to reference imaging. An additional external independent perfusion analysis can represent an additional step on the way to less examiner dependency, also with the use of artificial intelligence [10, 11].

CEUS with sulphur-hexafluoride microbubbles is a dynamic imaging technique down to the level of tumour capillaries [5]. The localization of tumour structures and the assessment of benign or malignant lesions is based on the following factors: wash-in kinetics, vascular patterns (regular vs. irregular) and wash-out kinetics (up to the late phase) [12]. Computed

tomography contrast agents are vascular and parenchymal and have different dynamics, whereas for MRI there are liver-specific contrast agents with vascular, parenchymal and RES-specific contrast. This can be particularly advantageous for the detection of smaller HCC foci [13-15]. Contrast enhanced ultrasound, on the other hand, is largely independent of renal function, which can be a decisive advantage in the case of altered creatinine clearance. Using second-generation ultrasound contrast agents, such as Sulphur-hexafluoride microbubbles (SonoVue®) (via intravenous bolus injection), CEUS allows dynamic recording of the microcirculation from the first 10 to 15 s (early arterial phase) to 5-6 min (late phase) and storage in DICOM-Cine sequences for different phases [5]. The detection of smaller tumour foci is based on using optimized technology multi-frequency probes, high frame rates and optimization of harmonic imaging of CHI (including PIHI and amplitude modulation). The new HiFR technique and perfusion analysis with external software offer an approach to this [2, 9, 10].

The characterization of benign foci of the liver is based on the detailed recording of the arterial microcirculation using CEUS (which is typical for benign lesions). Regular perfusion patterns: nodular enhancement from the edge in haemangiomas; spoked wheel pattern from the centre to the edge in FNH; spoked wheel pattern from the edge to the centre in adenomas [5, 15-17]. In complicated cysts that are reactively altered, a narrow septal contrast enhancement is found in septa < 2 mm. HiFR CEUS is sometimes superior to other diagnostic techniques (e.g. contrast enhanced CT or contrast enhanced MRI) in terms of recognisability for the contrast agent patterns described. CEUS can therefore serve as meaningful reference imaging. If biopsies are necessary as part of the diagnosis, it is recommended that a CEUS examination be carried out first in order to obtain optimum knowledge of the size, number and nature of possible lesions.

Using HiFR CEUS and perfusion analysis with the VueBox®, the typical contrast agent behavior could be derived in all cases of benign liver lesions from the edge to the center (e.g. FNH), nodular (e.g. hemangiomas) and from the center to the edge in the sense of a spoke wheel pattern (e.g. FNH) in a diagnosis-guiding manner. The contrast agent uptake increased in the late phase (up to 5 minutes). The contrast centre image was as follows: in typical haemangiomas it was complete; in thrombosed atypical haemangiomas a central depression remained in some cases; in typical cases of FNH a central scar was visible.

Typical for the perfusion analysis of malignant lesions was an arterial irregular accumulation of contrast medium in the HiFR CEUS and a wash-out beginning in the portal venous phase which was increasing towards the late phase. After correlation with CT/MRI there was reliable detection in all cases of colorectal metastases, but with irregular marginal vascularisation. However, it was possible to delineate the metastases with high image quality from as little as 5 mm in diameter using the wash-out in the portal venous phase after 50 s up to 5-6 min (late phase). The image quality was sometimes better than CT and achieved that of MRI with liver-specific contrast agent in almost all cases. In cases of small septate cysts up to 10 mm in diameter, HiFR

CEUS proved to be superior to CT for differentiation from metastases.

In malignant lesions, irregular hypervascularization is found in the arterial phase [e.g. in HCC, CCC, neuroendocrine tumours (NET) or NET foci] or in an irregular marginal vascularization (e.g. in metastases - especially colorectal) [5]. The use of HiFR CEUS can also be advantageous for detecting this irregular microvascularization. This also applies for the characterization of tumour cysts (with irregular septa > 3 mm) and tumour nodules. Particularly in smaller lesions (maximum diameter of 10 mm) the detection of irregular microvascularization could be decisive in the differentiation of regenerative nodules, dysplastic foci or HCC findings [4,18,19]. A high-resolution contrast agent mode such as HiFR CEUS is therefore crucial for determining the exact tumour entity.

To characterize a malignant lesion, it is crucial to record the dynamic wash-out kinetics over time. In metastases, this often begins in the portal venous phase (after 50 to 90 s), in CCC in the late portal venous phase and in HCC often only after 3 min, but can also only be recognizable in the late phase after 5 min. Independent perfusion analysis is also helpful in this case [20-22].

High-resolution CEUS techniques, such as the HiFR, are required to detect late washout behaviour. This applies in particular to small malignant tumour foci (diameter less than 10 mm). Under optimal acoustic conditions, CEUS can achieve a sensitivity comparable to contrast enhanced MRI [4, 5, 8].

Typical for the perfusion analysis of scarring changes after ablation (MWA) or postoperatively in CEUS was the lack of contrast enhancement from the arterial to the late phase. Typical for marginal recurrences are: irregular nodular accumulation at the margins and a washout of these nodular tumour parts (which starts in the portal-venous phase).

The defects could be described correctly in all cases using the HiFR CEUS technique. The same was applied to the description of postoperative defects with locally reduced fat content. In these cases, the hypoechoic areas in the B-scan appear garland-shaped with a wavy border. MRI examinations or a 2-phase multislice CT served as a reference [23].

When assessing vascular changes with CEUS, the decisive factor is the extent to which reduced perfusion (e.g. in infarcts, behind tumours), increased blood flow (e.g. in hyperaemia, micro/macro shunts) or tumour thromboses (including the passage of microbubbles into the thrombus) can be detected. In Osler's disease, signs of hepatic changes include elongation and dilatation of the hepatic artery (A hepatica) with early contrasting (often < 10 s), rapid contrasting of the portal vein (V portae through shunts, < 40 s) and the hepatic veins (< 50 s) [24-26]. Infarcts and scars show an avascular wedge-shaped pattern including typical perfusion changes.

Post-operative or post-ablative defects after interventions such as RFA, MWA or IRE may appear similar. Tumour recurrences often lead to irregular nodular marginal changes, arterially hyper-vascularized with wash-out in the late phase [27-30]. HiFR CEUS can prove to be useful in imaging micro-shunts or smaller tumour foci as well as high-resolution penetration of microbubbles into possible tumour thromboses.

However, there are limitations to the CEUS examination, even with HiFR. The clear dependence on the examiner's practical experience, the influence of a deep localization of possible foci, liver parenchymal changes, ascites, liver fibrosis or unfavorable ultrasound conditions (e.g. air overlay, obesity or poor compliance) should be emphasized [5]. In some cases, HiFR can make it easier to visualize the relevant findings.

Atypical partially thrombosed hemangiomas can be difficult to diagnose as the central thrombus may indicate a partial wash-out [5, 8, 31, 32]. This also applies to adenomas with central fat components or necrosis. In smaller NET lesions, a wash-out indicating malignancy may be absent, which can make differentiation from FNH or adenomas more difficult. The central scar of the FNH cannot always be imaged. After chemotherapy, partial necrosis can occur in metastases, which appear avascular. Partial avascular necrosis also occurs after TACE of malignant liver tumours [29, 33-35]. Under favorable acoustic conditions, HiFR CEUS perfusion imaging can image these partial necroses with a high level of detail.

## CONCLUSIONS

The extent to which HiFR with perfusion analysis makes it possible to achieve a higher diagnostic certainty than other CEUS modalities must be the aim of further studies, prospective and multicenter if possible, comparable to the DEGUM studies.

**Conflicts of interest:** None to declare.

**Authors' contributions:** L.P. and E.M.J. conceived the study. E.M.J. and F.J. designed the methodology. E.M.J. and L.P. collected the data. E.M.J. and F.J. performed the formal analysis. E.M.J., C.S. and U.K. drafted the manuscript. F.J. revised the paper. E.M.J. and F.J. supervised the study. All the authors read and approved the final version of the manuscript.

## REFERENCES

1. Jung EM, Dong Y, Jung F. Current aspects of multimodal ultrasound liver diagnostics using contrast-enhanced ultrasonography (CEUS), fat evaluation, fibrosis assessment, and perfusion analysis - An update. *Clin Hemorheol Microcirc* 2023;83:181-193. doi:[10.3233/CH-239100](https://doi.org/10.3233/CH-239100)
2. Jung EM, Moran VO, Engel M, Krüger-Genge A, Stroszczyński C, Jung F. Modified contrast-enhanced ultrasonography with the new high-resolution examination technique of high frame rate contrast-enhanced ultrasound (HiFR-CEUS) for characterization of liver lesions: First results. *Clin Hemorheol Microcirc* 2023;83:31-46. doi:[10.3233/CH-221449](https://doi.org/10.3233/CH-221449)
3. Zhao Q, Ji Z, Chen Y, et al. Contrast-enhanced ultrasound features of hepatic sarcomatoid carcinoma different from hepatocellular carcinoma. *Clin Hemorheol Microcirc* 2024;87:55-65. doi:[10.3233/CH-231944](https://doi.org/10.3233/CH-231944)
4. Schellhaas B, Bernatik T, Bohle W, et al. Contrast-Enhanced Ultrasound Algorithms (CEUS-LIRADS/ESLAP) for the Noninvasive Diagnosis of Hepatocellular Carcinoma - A Prospective

- Multicenter DEGUM Study. *Ultraschall Med* 2021;42:178-186. doi:10.1055/a-1198-4874
5. Dietrich CF, Nolsøe CP, Barr RG, et al. Guidelines and Good Clinical Practice Recommendations for Contrast Enhanced Ultrasound (CEUS) in the Liver - Update 2020 - WFUMB in Cooperation with EFSUMB, AFSUMB, AIUM, and FLAUS. *Ultraschall Med* 2020;41:562-585. doi:10.1055/a-1177-0530
  6. Laugesen NG, Nolsøe CP, Rosenberg J. Clinical Applications of Contrast-Enhanced Ultrasound in the Pediatric Work-Up of Focal Liver Lesions and Blunt Abdominal Trauma: A Systematic Review. *Ultrasound Int Open* 2017;3:E2-E7. doi:10.1055/s-0042-124502
  7. Sidhu PS, Cantisani V, Dietrich CF, et al. The EFSUMB guidelines and recommendations for the clinical practice of contrast-enhanced ultrasound (CEUS) in Non-Hepatic Applications: Update 2017 (Long Version). *Ultraschall Med* 2018;39:e2-e44. doi:10.1055/a-0586-1107
  8. Barr RG, Wilson SR, Lyshchik A, et al. Contrast-enhanced Ultrasound- State of the Art in North America: Society of Radiologists in Ultrasound White Paper. *Ultrasound Q* 2020;36(4S Suppl 1):S1-S39. doi:10.1097/RUQ.0000000000000515
  9. Giangregorio F, Garolfi M, Mosconi E, et al. High frame-rate contrast enhanced ultrasound (HIFR-CEUS) in the characterization of small hepatic lesions in cirrhotic patients. *J Ultrasound* 2023;26:71-79. doi:10.1007/s40477-022-00724-w
  10. Li N, Hu Z, Liu Y, et al. Dynamic contrast-enhanced ultrasound characteristics of renal tumors: VueBox™ quantitative analysis. *Clin Hemorheol Microcirc* 2023;85:341-354. doi:10.3233/CH-231750
  11. Hu HT, Wang W, Chen LD, et al. Artificial intelligence assists identifying malignant versus benign liver lesions using contrast-enhanced ultrasound. *J Gastroenterol Hepatol* 2021;36:2875-2883. doi:10.1111/jgh.15522
  12. Wang H, Guo W, Yang W, et al. Computer-Aided Color Parameter Imaging of Contrast-Enhanced Ultrasound Evaluates Hepatocellular Carcinoma Hemodynamic Features and Predicts Radiofrequency Ablation Outcome. *Ultrasound Med Biol* 2022;48:1555-1566. doi:10.1016/j.ultrasmedbio.2022.04.002
  13. Chiorean L, Tana C, Braden B, et al. Advantages and Limitations of Focal Liver Lesion Assessment with Ultrasound Contrast Agents: Comments on the European Federation of Societies for Ultrasound in Medicine and Biology (EFSUMB) Guidelines. *Med Princ Pract* 2016;25:399-407. doi:10.1159/000447670
  14. Meitner-Schellhaas B, Jesper D, Goertz RS, Zundler S, Strobel D. Washout appearance of hepatocellular carcinomas using standardized contrast-enhanced ultrasound (CEUS) including an extended late phase observation - Real-world data from the prospective multicentre DEGUM study. *Clin Hemorheol Microcirc* 2023;84:413-424. doi:10.3233/CH-231740
  15. Beyer LP, Wassermann F, Pregler B, et al. Characterization of Focal Liver Lesions using CEUS and MRI with Liver-Specific Contrast Media: Experience of a Single Radiologic Center. *Ultraschall Med* 2017;38:619-625. doi:10.1055/s-0043-105264
  16. Huang JY, Li JW, Lu Q, et al. Diagnostic Accuracy of CEUS LI-RADS for the Characterization of Liver Nodules 20 mm or Smaller in Patients at Risk for Hepatocellular Carcinoma. *Radiology* 2020;294:329-339. doi:10.1148/radiol.2019191086
  17. Şirli R, Sporea I, Popescu A, et al. Contrast-enhanced ultrasound for the assessment of focal nodular hyperplasia - results of a multicentre study. *Med Ultrason* 2021;23:140-146. doi:10.1152/mu-2912
  18. van der Pol CB, McInnes MDF, Salameh JP, et al. CT/MRI and CEUS LI-RADS Major Features Association with Hepatocellular Carcinoma: Individual Patient Data Meta-Analysis. *Radiology* 2022;302:326-335. doi:10.1148/radiol.239005
  19. Wilson SR, Lyshchik A, Piscaglia F, et al. CEUS LI-RADS: algorithm, implementation, and key differences from CT/MRI. *Abdom Radiol (NY)* 2018;43:127-142. doi:10.1007/s00261-017-1250-0
  20. Wang P, Nie F, Dong T, Yang D, Liu T, Wang G. Diagnostic Value of CEUS LI-RADS Version 2017 in Differentiating AFP-Negative Hepatocellular Carcinoma from Other Primary Malignancies of the Liver. *Diagnostics (Basel)* 2021;11:2250. doi:10.3390/diagnostics11122250
  21. Caraianni C, Boca B, Bura V, Sparchez Z, Dong Y, Dietrich C. CT/MRI LI-RADS v2018 vs. CEUS LI-RADS v2017-Can Things Be Put Together? *Biology (Basel)* 2021;10:412. doi:10.3390/biology10050412
  22. Cheng MQ, Huang H, Ruan SM, et al. Complementary Role of CEUS and CT/MRI LI-RADS for Diagnosis of Recurrent HCC. *Cancers (Basel)* 2023;15:5743. doi:10.3390/cancers15245743
  23. Zheng R, Zhang X, Liu B, et al. Comparison of non-radiomics imaging features and radiomics models based on contrast-enhanced ultrasound and Gd-EOB-DTPA-enhanced MRI for predicting microvascular invasion in hepatocellular carcinoma within 5 cm. *Eur Radiol* 2023;33:6462-6472. doi:10.1007/s00330-023-09789-5
  24. Schelker RC, Andorfer K, Putz F, Herr W, Jung EM. Identification of two distinct hereditary hemorrhagic telangiectasia patient subsets with different hepatic perfusion properties by combination of contrast-enhanced ultrasound (CEUS) with perfusion imaging quantification. *PLoS One* 2019;14:e0215178. doi:10.1371/journal.pone.0215178
  25. Schelker RC, Barreiros AP, Hart C, Herr W, Jung EM. Macro- and microcirculation patterns of intrahepatic blood flow changes in patients with hereditary hemorrhagic telangiectasia. *World J Gastroenterol* 2017;23:486-495. doi:10.3748/wjg.v23.i3.486
  26. Möller K, Tscheu T, De Molo C, et al. Comments and illustrations of the WFUMB CEUS liver guidelines: rare congenital vascular pathology. *Med Ultrason* 2022;24:461-472. doi:10.1152/mu-3879
  27. Kloth C, Kratzer W, Schmidberger J, Beer M, Clevert DA, Graeter T. Ultrasound 2020 – Diagnostics & Therapy: On the Way to Multimodal Ultrasound: Contrast-Enhanced Ultrasound (CEUS), Microvascular Doppler Techniques, Fusion Imaging, Sonoelastography, Interventional Sonography. *Rofo* 2021;193:23-32. doi:10.1055/a-1217-7400
  28. Jung EM, Stroszczyński C, Jung F. Advanced multimodal imaging of solid thyroid lesions with artificial intelligence-optimized B-mode, elastography, and contrast-enhanced ultrasonography parametric and with perfusion imaging: Initial results. *Clin Hemorheol Microcirc* 2023;84:227-236. doi:10.3233/CH-239102
  29. Faccia M, Garcovich M, Ainora ME, et al. Contrast-Enhanced Ultrasound for Monitoring Treatment Response in Different Stages of Hepatocellular Carcinoma. *Cancers (Basel)* 2022;14:481. doi:10.3390/cancers14030481
  30. Russell G, Strnad BS, Ludwig DR, et al. Contrast-Enhanced Ultrasound for Image-Guided Procedures. *Tech Vasc Interv Radiol* 2023;26:100913. doi:10.1016/j.tvir.2023.100913
  31. Safai Zadeh E, Prosch H, Ba-Ssalamah A, et al. Contrast-enhanced ultrasound of the liver: basics and interpretation of common focal lesions. *Rofo* 2024;196:807-818. doi:10.1055/a-2219-4726
  32. Quarato CMI, Feragalli B, Lacedonia D, et al. Contrast-Enhanced Ultrasound in Distinguishing between Malignant and Benign Peripheral Pulmonary Consolidations: The Debated Utility of the Contrast Enhancement Arrival Time. *Diagnostics (Basel)* 2023;13:666. doi:10.3390/diagnostics13040666
  33. Lee CC, Hwang JI, Chang KH, et al. Comparison of contrast-enhanced ultrasonography and MRI results obtained by expert and

- novice radiologists indicating short-term response after transarterial chemoembolisation for hepatocellular carcinoma. *Clin Radiol* 2024;79:e73-e79. doi:[10.1016/j.crad.2023.09.015](https://doi.org/10.1016/j.crad.2023.09.015)
34. Tai CJ, Huang MT, Wu CH, et al. Contrast-Enhanced Ultrasound and computed Tomography Assessment of Hepatocellular Carcinoma after Transcatheter Chemo-Ambolization: A Systematic Review. *J Gastrointestin Liver Dis* 2016;25:499-507. doi:[10.15403/jgld.2014.1121.254.tai](https://doi.org/10.15403/jgld.2014.1121.254.tai)
35. Sporea I, Sandulescu DL, Sirli R, et al. Contrast-Enhanced Ultrasound for the Characterization of Malignant versus Benign Focal Liver Lesions in a Prospective Multicenter Experience - The SRUMB Study. *J Gastrointestin Liver Dis* 2019;28:191-196. doi:[10.15403/jgld-180](https://doi.org/10.15403/jgld-180)